

Supporting Information

A smart-bottle humidifier assisted air-processed CuSCN inorganic hole extraction layer towards highly-efficient, large-area and thermally-stable perovskite solar cells

Sawanta S. Mali,¹ Jyoti V. Patil¹ and Chang Kook Hong^{1*}

¹ *Polymer Energy Materials Laboratory, School of Advanced Chemical Engineering, Chonnam National University, Gwangju-S. Korea 61186*

**Correspondence to: sawantasolar@gmail.com (SSM), hongck@jnu.ac.kr (CKH)*

Table of contents

I. Materials and Methods

II. Supplementary Text

III. Supplementary Figures

Fig. S1. Optical images of Smart-bottle humidifier and its neck

Fig. S2 Schematic representation of experimental assembly used for CuSCN deposition.

Fig. S3 2D and 3D AFM micrographs of CuSCN coating from 5mg/ml concentration on perovskite layer.

Fig. S4 XRD pattern of perovskite thin film deposited on mp-TiO₂ substrate.

Fig. S5 XRD pattern of β -CuSCN thin film deposited on glass substrate

Fig. S6 Cross sectional SEM micrograph of spiro-MeOTAD based PSC used in the present study for comparison and its schematic representation. The spiro-MeOTAD layer shows formation of pin-holes.

Fig. S7 Hysteresis analysis of spiro-MeOTAD based PSC used in the present study for comparison

Fig. S8 The steady-state photocurrent output profile for spiro-MeOTAD and CuSCN based PSCs.

Fig. S9 Hole mobility: J–V characteristics of space-charge-limited current (SCLC) of CuSCN and spiro-MeOTAD HTMs. Relatively low threshold voltages indicate that these SCLC devices have ohmic contact.

Fig. S10 Thermal stability. Thermal stability of CuSCN and CuSCN/rGO i-HELs based perovskite solar cells recorded at 85°C. Note: Both devices were encapsulated with PMMA solution before thermal study and kept in vacuum oven in dark at 85 ±1°C at - 0.01 mPa vacuum.

Fig. S11 Thermal stability after 1000 hours. Thermal stability of CuSCN and CuSCN/rGO i-HELs based perovskite solar cells recorded at 85°C. Note: Both devices were covered with PMMA solution before thermal study and kept in only in normal oven in dark at 85 ±1°C.

Figure S12 Thermal stability testing. Optical images of CuSCN i-HEL based PSCs at different time interval

Figure S13 FT-IR spectra of diethyl sulfide solution, CuSCN dissolved in DES, perovskite/CuSCN device at different time interval.

Table S1 Solar cell parameters extracted from J-V curves of the CuSCN based HEL deposited from different solution concentration.

Table S2 TRPL lifetime measurements of perovskite absorber with different interfaces. Weight fraction calculated from amplitude at particular lifetime decay.

Table S3 Solar cell parameters extracted from J-V curves recorded under forwards and reverse scan direction for CuSCN HEL and spiro-MeOTAD HTM based champion devices.

Table S4 Literature survey of highly-efficient PSCs based on different HTM and ETLs

I. Materials and Methods

Materials

All of the chemicals and materials were purchased and used without further purification.

Materials including solvents (N, N-Dimethylformamide (DMF), Dimethyl sulfoxide (DMSO), diethyl sulfide (98%), PbI_2 (99%) and Copper(I) thiocyanate (CuSCN) (>99%) were purchased from Sigma-Aldrich and used as received. Hydroiodic acid (aqueous, 57 wt %, Sigma-Aldrich) to a solution of methylamine (aqueous, 40 wt %, TCI Chemicals), formamidine acetate (Sigma-Aldrich) was used for preparation of MAI, FAI. For CuSCN and rGO deposition, we used the commercial Smart Bottle Humidifier (dimension Height: 180 mm, Width: 56.8 mm, Upper neck: 9 mm, Weight: 93.3 g Voltage: DC 5V Power: 2W, Capacity of solution: 180 ml (max). More details can be found Web site: www.enbow.co.kr. For power source, we used MI power bank, 10,000 mAh. <https://www.mi.com/en/pb10000/>

Methods

Preparation of Electron transport layer (ETL)

Laser-patterned FTO-coated glass substrates (TEC-8, Pilkington) were ultrasonically cleaned in an alkaline aqueous solution, rinsed with deionized water, acetone, ethanol and then treated with UV-ozone for 15 min. Nearly 50-nm-thick compact blocking TiO_2 (BI- TiO_2) layer was deposited on the FTO substrates by first spin coating the TTIP precursor solution TiO_2 from mild acidic ethanol solvent followed by annealing at 450 °C. After cooling the substrates to room temperature, they were treated with the 0.04M TiCl_4 aqueous solution for 30 min at 70 °C, then rinsed with deionized water and dried at 500 °C for 20 min. Nearly, 200nm mp- TiO_2 layer was composed of the 20-nm-sized particles and deposited by spin coating a commercial TiO_2 paste (Dyesol DSL-30NR-T, Dyesol) diluted in ethanol (5.5:1 weight ratio) at 4000 r.p.m. for 15 s

with ramp rate 2000 rpm s⁻¹. After drying at 120 °C, the TiO₂ films were gradually heated to 500 °C, baked at this temperature for 15 min and then cooled to room temperature. The mesoporous deposited film was again treated with TiCl₄ followed by sintering. The Li- treatment was achieved by spin coating of 200 µl of LiTFSI in acetonitrile (10 mgml⁻¹) at 3000 rpm followed by sintering at 450 °C for 30 min in air. When furnace temperature cooled at 150 °C, the Li treated mp-TiO₂ electrodes were transferred in glove box for perovskite deposition.

Synthesis of the perovskite precursors and their solution

The FAI, MABr were synthesized as per our reports.¹⁶ For Cs_{0.05}FA_{0.81}MA_{0.14}PbI_{2.55}Br_{0.45} precursors was synthesized by reacting FAI, MABr, PbI₂, PbBr₂ and CsI powder with desired amount in DMF/DMSO (4:1 v/v%) solution. Note that 1.5 M CsI precursor stock solution was initially prepared in DMSO solvent followed by addition of proper volume addition in (FAPbI₃)_{0.85}(MAPbBr₃)_{0.15} precursor. The clear filtered yellow solution was spin coated on the top of the FTO/mp-TiO₂ electrode by a consecutive two-step spin coating process at 1,000 and 6,000 rpm for 10 and 30 s, respectively. 100 µl of chlorobenzene was drop-cast during the second spin-coating step and annealed at 100°C for 90 min.

Preparation of conventional spiro-MeOTAD based HTM

The hole transport material (HTM) was prepared by as per our previous report.^[1,2] The 72 mg 2,2',7,7'-tetrakis-(N, N-di-p-methoxyphenyl-amine)-9,9'-spirobifluorene (spiro-MeOTAD, Merck) dissolved in 1mL chlorobenzene (99.8%, Aldrich) with addition of 37.5 µL bis(trifluoromethane) sulfonimide lithium salt (LiTFSI, 99.95%, Aldrich) (170mgml⁻¹) in acetonitrile, 20 µl tris(2-(1Hpyrazol-1-yl)-4-tert-butylpyridine)-cobalt(III) tris(bis(trifluoromethylsulfonyl) imide) (FK 209, from Dyenamo) (300 mgml⁻¹, ACN) and 17.5 µL 4-tert-butylpyridine (TBP, 96%, Aldrich). The prepared spiro-MeOTAD

HTM solution was spin-coated on the FTO/mp-TiO₂/perovskite substrate at 3,000 r.p.m for 30s. Then the substrates were transferred to a vacuum chamber and evacuated to a pressure of 2×10^{-6} mbar. For the counter electrode, a 80 nm thick Au contacts were deposited on the top of the HTM over layer by a thermal evaporation (growth rate $\sim 0.5 \text{ \AA/s}$). The active area of this electrode was fixed at 0.09 cm^2 . An active area was calculated as per gold and laser pattern cross-sectional area. The exact illumination to the active area was fixed by attaching metal shadow mask from back side during measurements.

Synthesis of CuSCN precursor:

Different precursor ratio 5, 10, 15, 20, 25 and 30 mg ml^{-1} CuSCN i-HEL in diethyl sulfide solution was prepared by continuous stirring for 30 min at room temperature. The cleared solution was used for deposition.

Synthesis of graphene oxide (GO):

Graphene oxide (GO) was prepared using modified Hummer's method while the reduced graphene oxide (rGO) was obtained by simply thermal annealing process at 550°C for 30min.^[3] The rGO interfacial layer was obtained by coating 1 mg/ml rGO (2 ml) solution in chlorobenzene followed by SBHA coating. For coating we have used 2 ml rGO/CB solution.

CuSCN deposition

For CuSCN deposition, we have used smart-bottle neck (Fig. S1) for CuSCN solution deposition. The 2 ml of precursor solution was filled in bottle neck and deposited on the FTO/TiO₂/Perovskite substrate by the as described in Fig. 1. The humidifier neck was connected to the portable power bank (MI 10,000 mAh) and 2 ml CuSCN solution was filled in the neck. The CuSCN deposition was taken in fume-hood in order to avoid skin, eye contact of diethyl-sulfide. During deposition the perovskite surface was continuously flush with dry nitrogen gas. Nine devices were kept on preheated hot plate ($15 \times 15 \text{ cm}^2$) for CuSCN deposition (See Fig. S2). The smart bottle neck is

about 10 cm far from the hot-plate surface and at an angle of 90°. The smart bottle neck is rapidly moved horizontally around in a single circle to cover the whole 10 × 10 cm² FTO/mp-TiO₂/Perovskite surface (9 devices were kept on hot plate). This cyclic movement is repeated until finishing the 2 ml solution within 4 min. The spraying rate was calculated and its nearly 0.5 ml min⁻¹. Finishing the solution usually takes about 4-5 min. Note: The DES inhalation is dangerous to health. Therefore, we have carried out these experiments, in Fume-Hood with proper masking and using hand-gloves. Please refer MSDS of DES solvent before use. Then the CuSCN coated devices left for additional 10 minutes at 95°C and used for gold deposition. The bottle-tip and substrate distant was kept fixed at 10 cm and the perovskite substrate was placed on a hot plate during deposition at 95 °C. In addition, rGO interfacial layer (1 mg/ml in chlorobenzene) was deposition before making Au contact. The deposition coating rate was calculated by the amount of CuSCN/diethyl sulfide solution quantity. In our case, the calculated rate was 0.5 ml/min. The thickness of CuSCN layer was controlled by deposition time and CuSCN concentration. After the final deposition, the coated CuSCN films were further backed at 80 °C for another 10 min with nitrogen flush. Similar procedure was adopted for rGO deposition. The devices were completed by deposited 80 nm Au contacts at 2 × 10⁻⁶ mbar vacuum onto the CuSCN layer through shadow masks defining two devices on one substrate by using thermal evaporation technique. The active area of all devices was 0.09 cm².

Characterizations

The morphological studied such as top-view and cross-sectional micrographs were recorded by a field emission scanning electron microscope (FESEM; S-4700, Hitachi). The structural analysis was done by X-ray diffraction (XRD) measurements using a D/MAX Ultima III XRD spectrometer (Rigaku, Japan) with Cu K line of 1.5410 Å. The surface morphology and RMS

values of CuSCN and perovskite thin films was obtained by using atomic force microscopy (XE-100 Advanced Scanning Probe Microscope, Park Systems). The photoluminescence (PL) spectra were measured using photoluminescence spectrometer ($f=0.5\text{m}$, Acton Research Co., Spectrograph 500i, USA), and an intensified CCD(PI-MAX3) (Princeton Instrument Co., IRY1024, USA). The DPSS (Diode pumped solid state) laser (Ekspla) with a wavelength of 266 nm and a power of 310 mW was utilized as an excitation source for PL measurement.

Photovoltaic studies

The perovskite devices were tested under standard testing conditions such as 100 mWcm^{-2} light intensity produced by solar simulator. The light intensity was adjusted to 1 sun intensity (100 mW cm^{-2}) through the use of an NREL-calibrated Si solar cell with a KG-5 filter. The external quantum efficiency (EQE) spectra were measured as a function of wavelength from 300 to 900 nm on the basis of a Spectral IPCE Measurement system K3100. The EQE spectra were normalized to the measured J–V current for accurate comparison. The EQE data were collected in the constant energy DC mode with a delay time of 10 ms and a light intensity of $50\text{ }\mu\text{Wcm}^{-2}$.

Device stability

The device stability was tested in air and after each measurements devices were stored in nitrogen filled glove box in dark (for spiro-MeOTAD) and vacuum oven (for CuSCN based) with PMMA coating. Please note that we made vacuum only -0.01Mpa that was needed to close the vacuum-oven door and avoid external moisture. For thermal stability, CuSCN based devices were coated with PMMA and kept in vacuum oven at $65 \pm 1\text{ }^\circ\text{C}$ and $85 \pm 1\text{ }^\circ\text{C}$ for each 25 devices. The measurements were carried out outside the vacuum chamber in ambient condition. For long term stability, spiro-MeOTAD and CuSCN HTM based devices were sealed with respectively

with Amisol sealant and PMMA encapsulation. The maximum power point of the encapsulated device for long term stability was monitored under AM1.5 G simulated light.

II. Supplementary text:

TRPL analysis

The TRPL decay profile data was fitted to a tri-exponential function of the form:^[4]

$$I(t) = I_0 + A_1 \exp\left(-\frac{t-t_0}{\tau_1}\right) + A_2 \exp\left(-\frac{t-t_0}{\tau_2}\right) + A_3 \exp\left(-\frac{t-t_0}{\tau_3}\right) \quad (\text{S1})$$

where, τ_1 , τ_2 and τ_3 are first, second and third order decay time, A_1 , A_2 and A_3 are respective weight factors of each decay channel. The average recombination lifetimes $\langle \tau_{\text{avg}} \rangle$ for respective samples were calculated from lifetime values and weight fraction amplitude values (%) using the following equation:^[5]

$$\langle \tau_{\text{avg}} \rangle = \frac{\sum_n A_n \tau_n^2}{\sum_m A_m \tau_m^2} \quad (\text{S2})$$

III. Figures

Fig. S1. Optical images of Smart-bottle humidifier and its neck

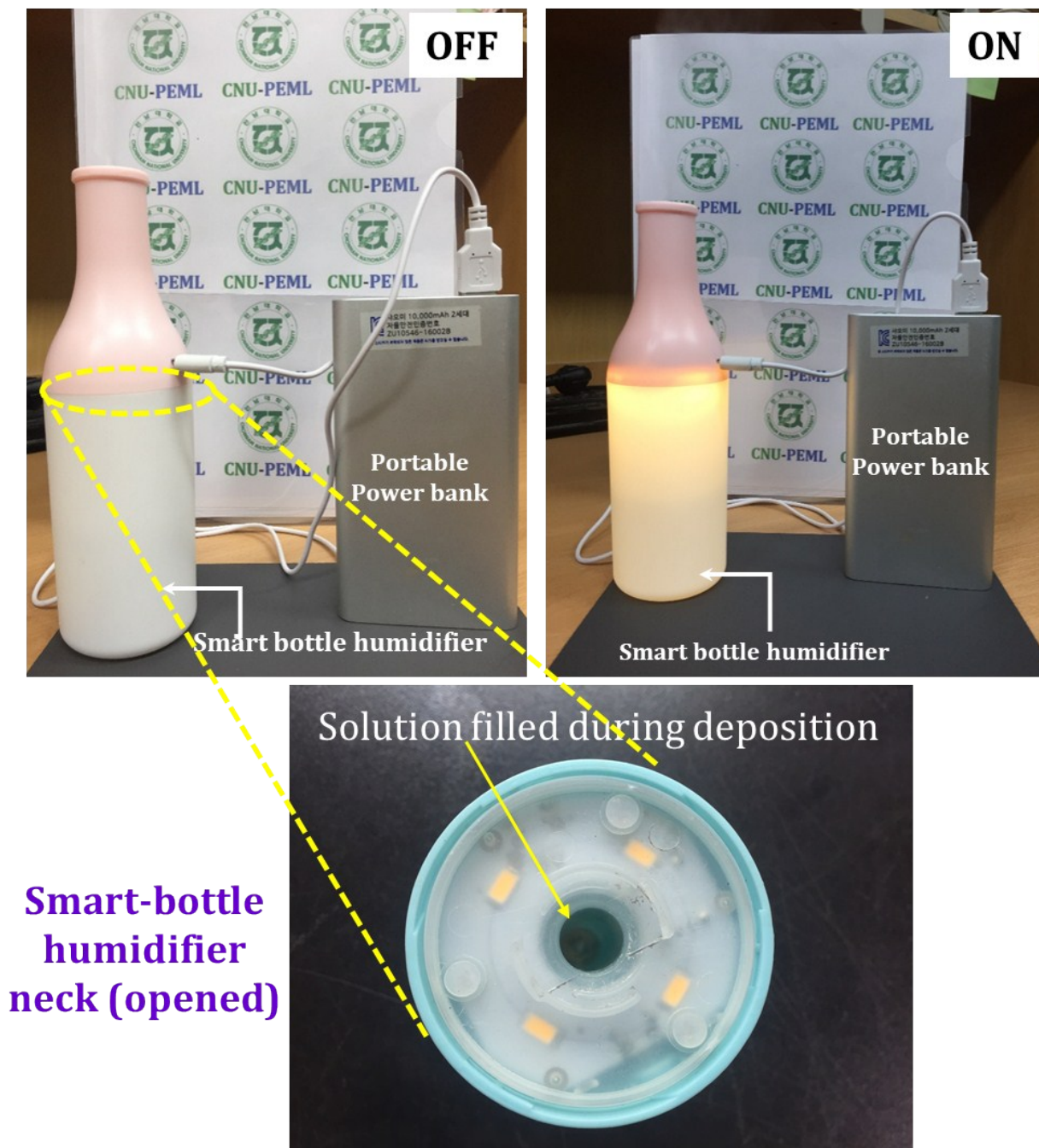


Fig. S2 Schematic representation of experimental assembly used for CuSCN deposition.

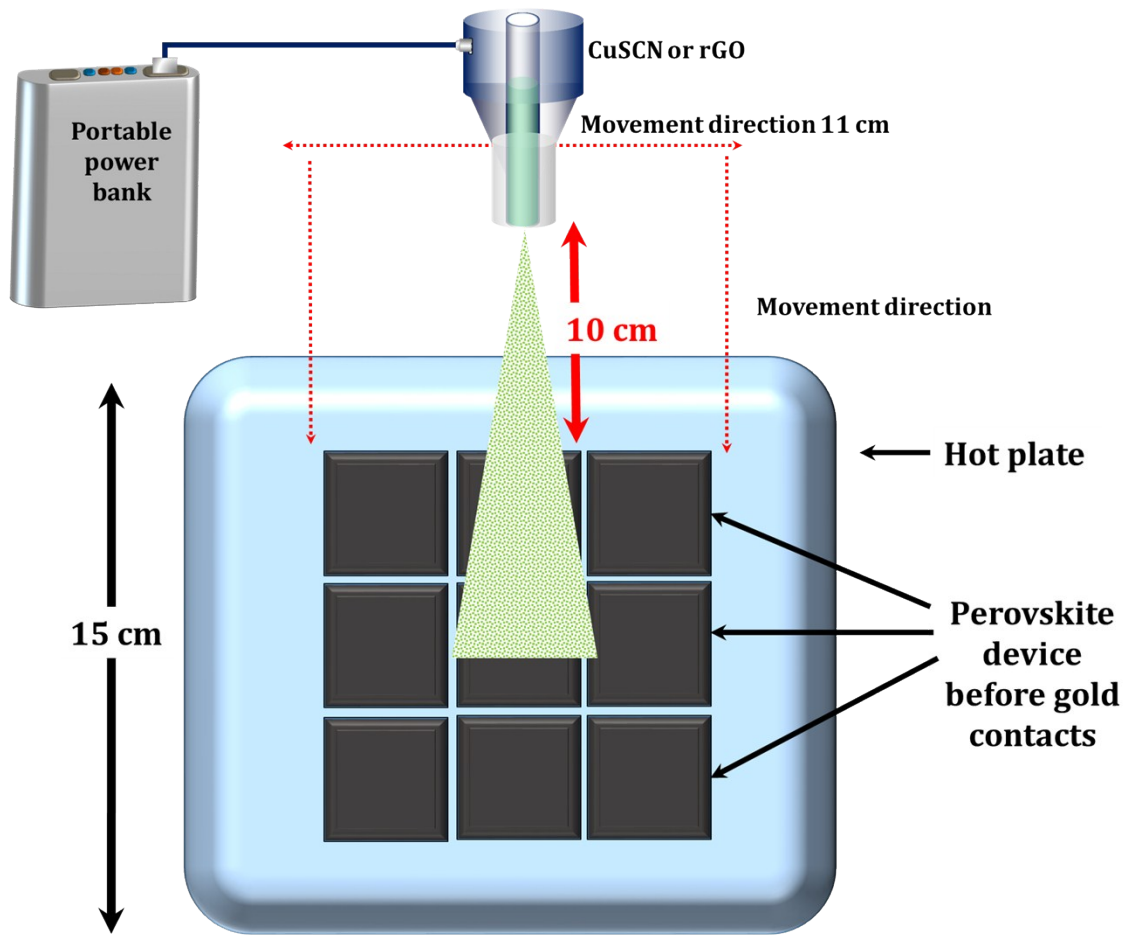


Fig. S3 2D and 3D AFM micrographs of CuSCN coating from 5mg/ml concentration on perovskite layer.

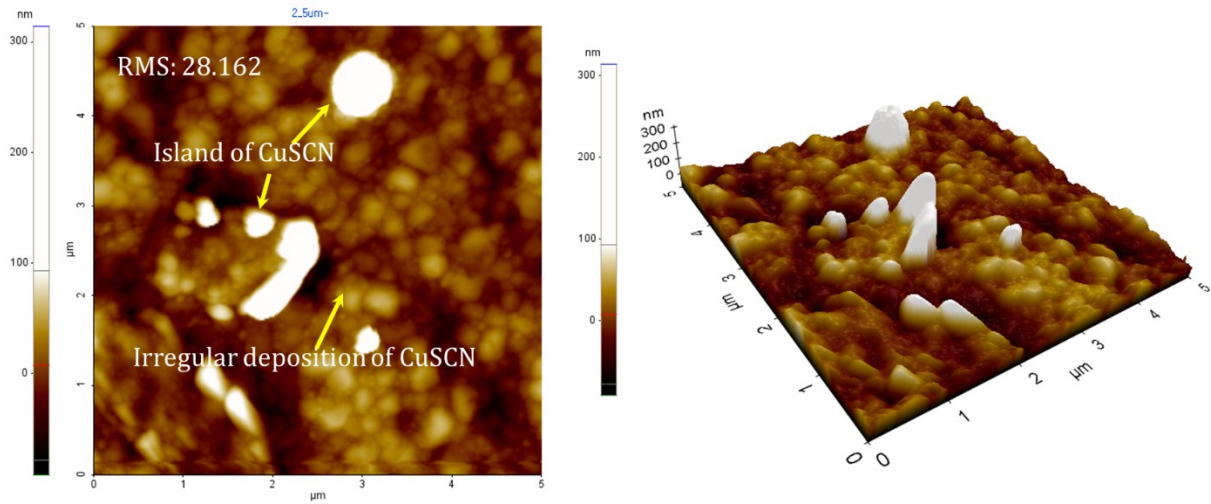


Fig. S4 XRD pattern of perovskite thin film deposited on mp-TiO₂ substrate.

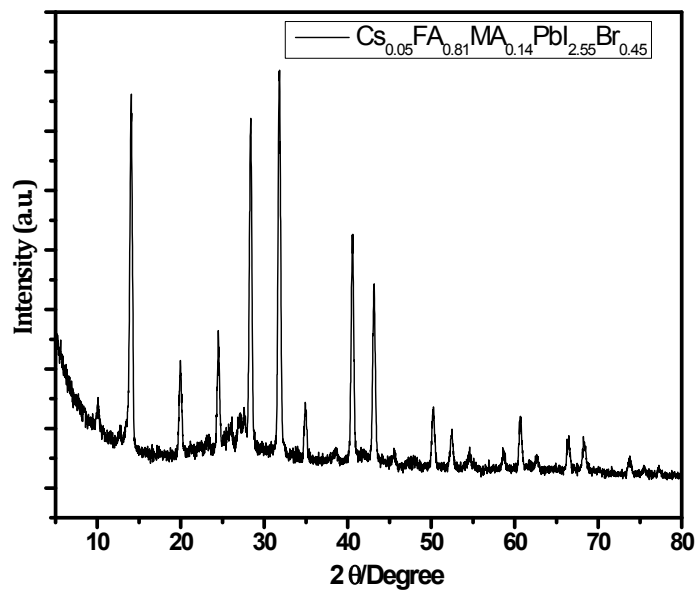


Fig. S5 XRD pattern of β-CuSCN thin film deposited on glass substrate

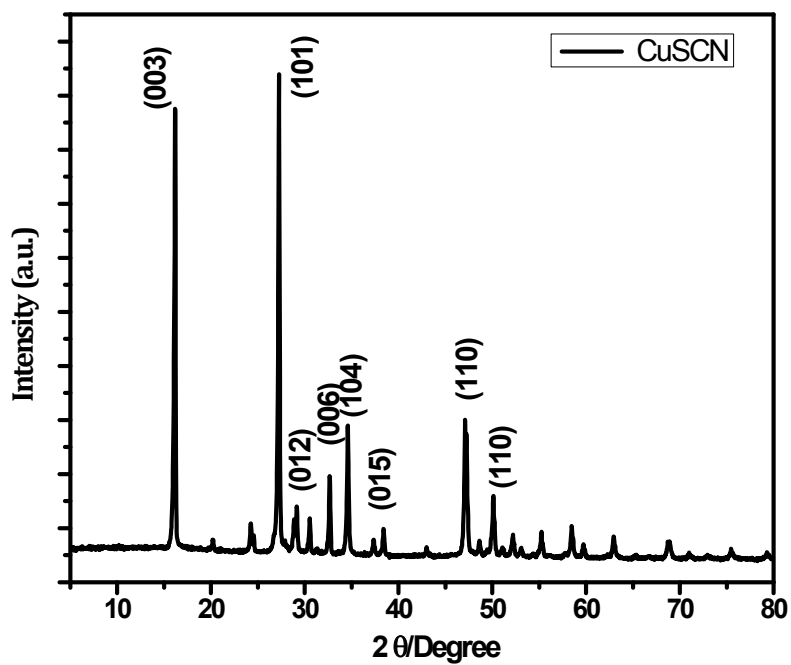


Fig. S6 Cross sectional SEM micrograph of conventional spiro-MeOTAD based PSC used in the present study for comparison and its schematic representation. The spiro-MeOTAD layer shows formation of pin-holes.

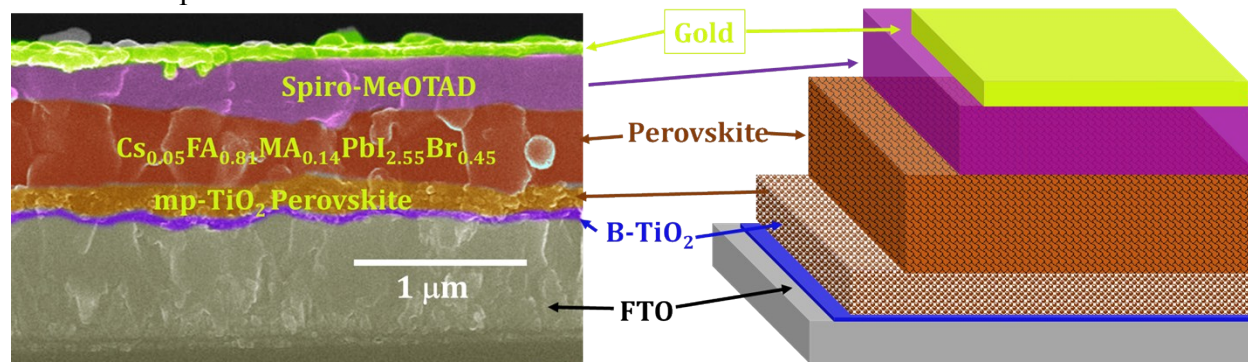


Fig. S7 Hysteresis analysis of spiro-MeOTAD based PSC used in the present study for comparison

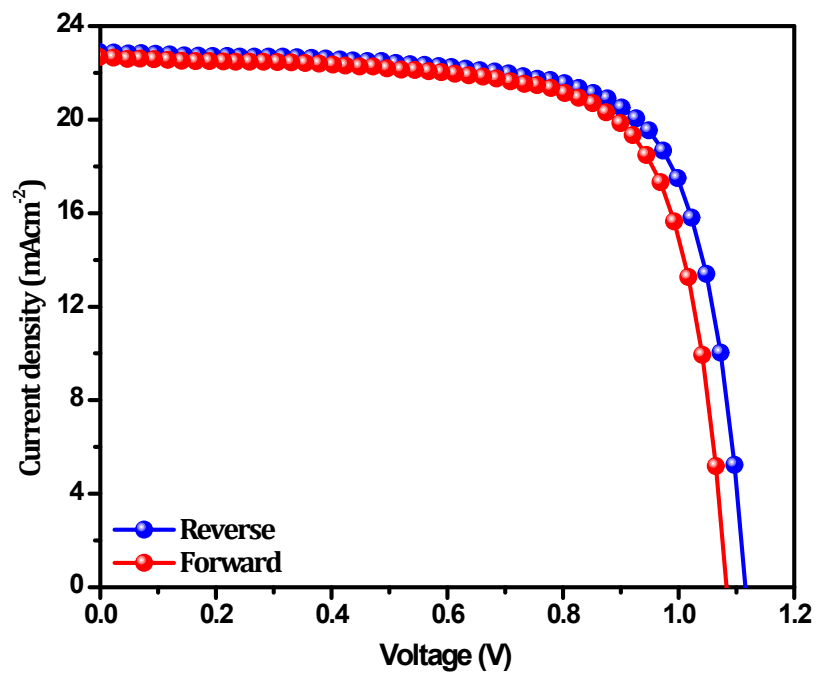
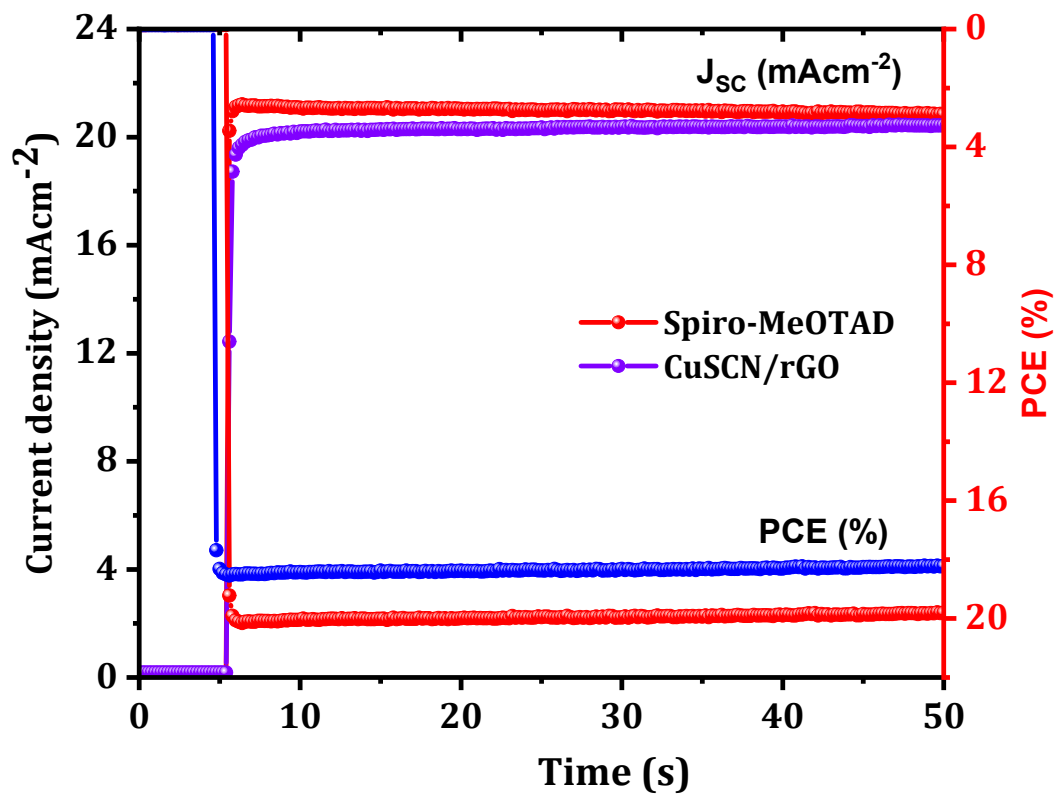


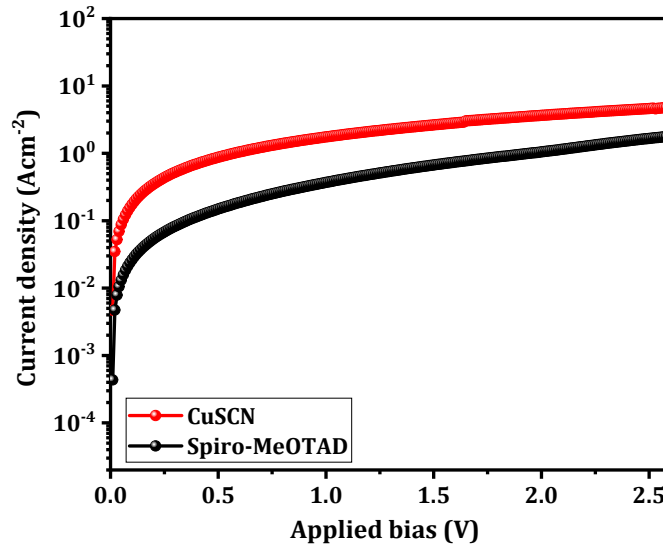
Fig. S8 The steady-state photocurrent output profile for spiro-MeOTAD and CuSCN based PSCs.



Hole mobility measurement by space-charge-limited current (SCLC)

In order to measure the hole mobility of spiro-MeOTAD and CuSCN HTL, we have fabricated hole-only devices. The ITO-coated glass substrate (15 Ω /sq, iTASCO) was washed carefully under ultrasonic irradiation using Helmanex soap, water, acetone, and ethanol for 15 min each step. The cleaned substrates were treated with UV/ozone for 15 min. A thin layer of PEDOT:PSS (Baytron AI 4083) was prepared onto the ITO surface by the spin-coating at 5000 rpm for 60 s). The PEDOT:PSS coated ITO substrate were heated at 200 $^{\circ}$ C for 10 min under ambient conditions. Then, hole transporting layers such as spiro-MeOTAD or CuSCN coated onto PEDOT:PSS layer from chlorobenzene or diethylsulfide solvent respectively. Finally, 30 nm Au was deposited on the film by thermal evaporation.

Fig. S9 J–V characteristics of space-charge-limited current (SCLC) of CuSCN and spiro-MeOTAD HTMs. Relatively low threshold voltages indicate that these SCLC devices have ohmic contact.



The hole mobilities in the films of materials were measured from the space-charge-limitation of current (SCLC) J–V characteristics obtained in the dark for hole-only devices. Hole mobilities were calculated using the Mott-Gurney law by fitting following Equation:

$$J(V) = \frac{9}{8} \varepsilon \varepsilon_0 \mu \frac{V^2}{d^3} \dots (S3)$$

where J is the current density, ε is permittivity of the materials (usually ~ 3 for organic semiconductors and 10 for CuSCN), ε_0 is the permittivity of free space (8.85×10^{-12} F/m), μ is the hole mobility, V is the applied voltage, and d is the thickness of the active layer.⁽⁶⁻⁸⁾

Fig. S10 Thermal stability. Thermal stability of CuSCN and CuSCN/rGO i-HELs based perovskite solar cells recorded at 85°C. Note: Both devices were encapsulated with PMMA solution before thermal study and kept in vacuum oven in dark at $85 \pm 1^\circ\text{C}$ at -0.01 mPa vacuum.

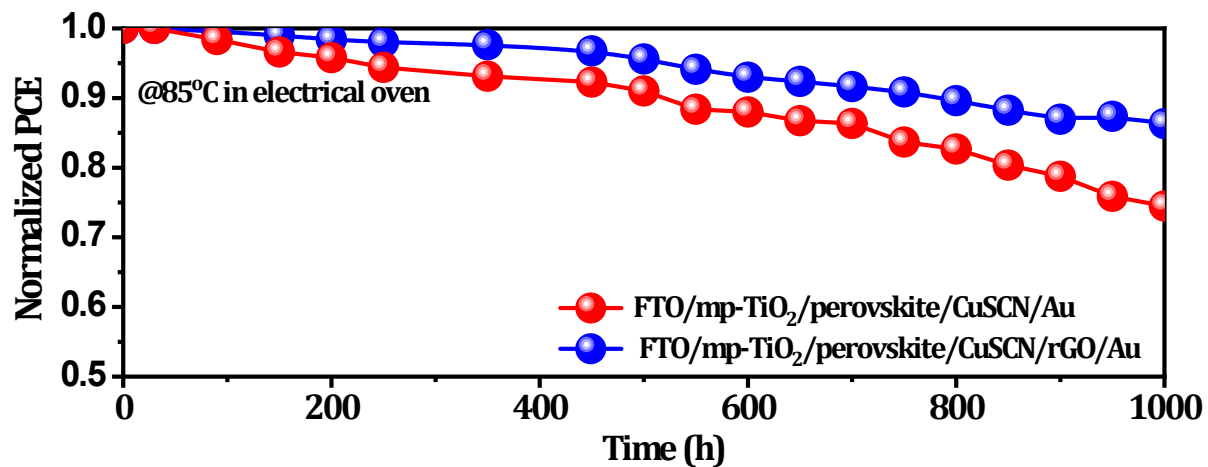


Fig. S11 Thermal stability after 1000 hours. Thermal stability of CuSCN and CuSCN/rGO i-HELs based perovskite solar cells recorded at 85°C. Note: Both devices were covered with PMMA solution before thermal study and kept in only in normal oven in dark at 85 ±1°C.

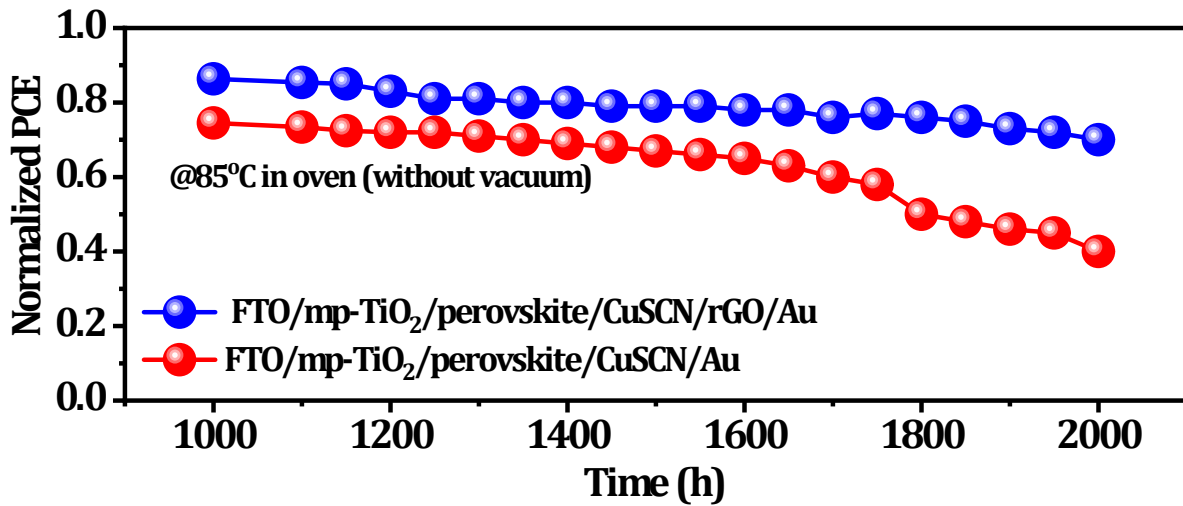


Figure S12 Thermal stability testing. Optical images of CuSCN i-HEL based PSCs at different time interval

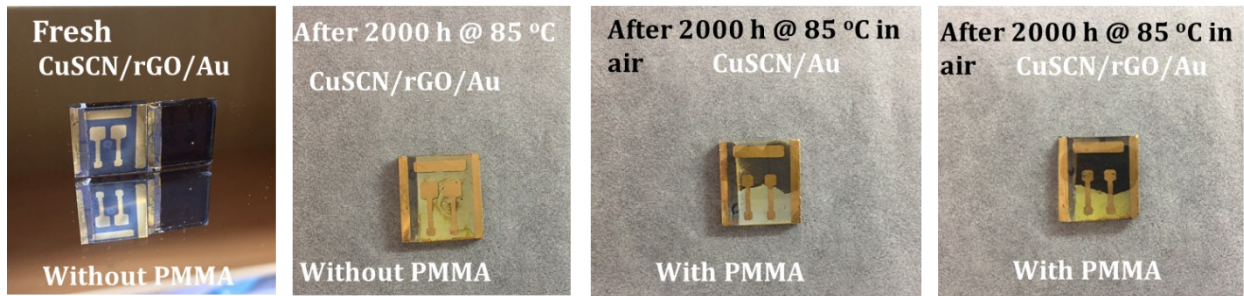


Figure S13 FT-IR spectra of diethyl sulfide solution, CuSCN dissolved in DES, perovskite/CuSCN device at different time interval.

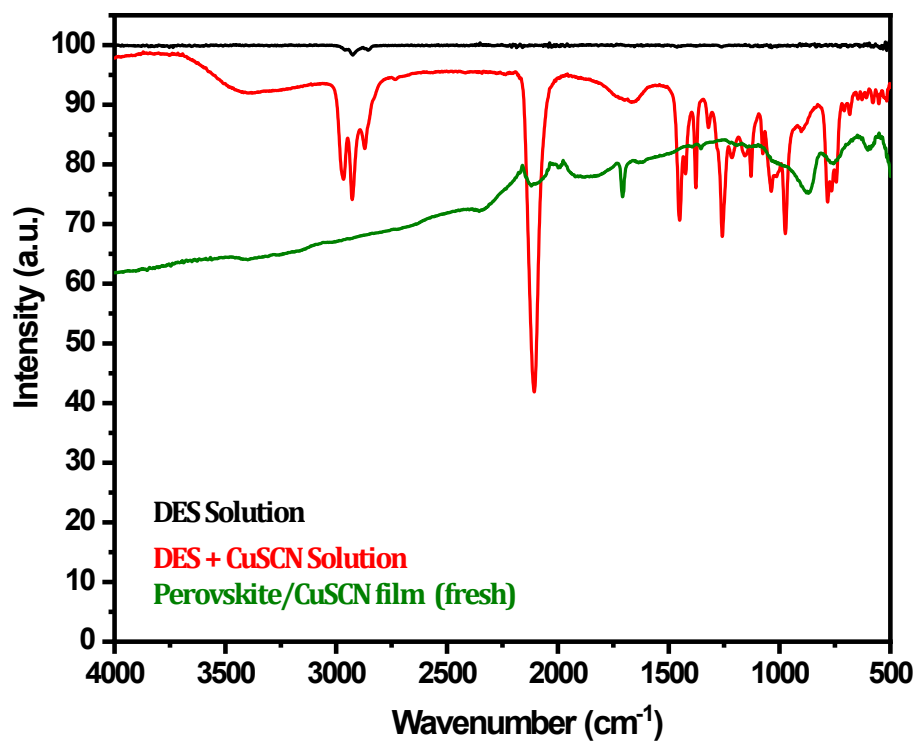


Table S1 Solar cell parameters extracted from J-V curves of the CuSCN based HEL deposited from different solution concentration.

CuSCN (mg/ml)	V_{oc} (V)	J_{sc} (mAcm⁻²)	FF (%)	PCE (%)
5	0.991	21.28	66.76	14.08
10	1.074	23.17	75.56	18.74
15	1.046	21.98	72.30	16.62
20	1.031	21.43	71.40	15.77
25	1.027	21.08	69.43	15.03
30	1.015	20.76	67.40	14.20
Conventional method	0.863	18.65	53.46	8.59
Spiro-MeOTAD	1.112	23.18	75.15	19.37

Table S2 TRPL lifetime measurements of perovskite absorber with different interfaces. Weight fraction calculated from amplitude at particular lifetime decay.

Perovskite/HEL	τ_1 (ns)	τ_2 (ns)	τ_3 (ns)	A₁*	A₂*	A₃*	<τ> (ns)
Perovskite/PMMA	295	12	71	0.0371	0.7323	0.2305	125
mp-TiO ₂ /Perovskite/spiro-MeOTAD	88	17	3.1	0.0262	0.3458	0.6268	44
mp-TiO ₂ /Perovskite /CuSCN	96	1.6	11	0.0255	0.7738	0.2006	30

Table S3 Solar cell parameters extracted from J-V curves recorded under forwards and reverse scan direction for CuSCN HEL and spiro-MeOTAD HTM based champion devices.

	Scan direction	V_{oc} (V)	J_{sc} (mAcm⁻²)	FF (%)	PCE (%)
CuSCN (10 mg/ml)	Reverse	1.074	23.17	75.56	18.74
	Forward	1.034	23.41	73.52	17.79
	Average	1.054	23.29	74.54	18.26
Spiro-MeOTAD	Reverse	1.112	23.18	75.15	19.37
	Forward	1.089	22.95	74.10	18.52
	Average	1.100	23.065	74.62	18.94

Supplimentary References:

1. S. S. Mali, C. S. Shim, C. K. Hong, *NPG Asia Materials* (2015) 7, e208,
2. S. S. Mali et al., *J. Mater. Chem. A*, 2017, 5, 12340
3. S. S. Mali et al., *J. Mater. Chem. A*, 2016, 4, 12158
4. J. R. Lakowicz, *Principles of Fluorescence Spectroscopy*, 3rd Ed., 2006, Springer
5. A. Sillen, Y. Engenborghs, The correct use of “Average” Fluorescence Parameters, *Photochemistry and Photobiology* 1998, 67(5):475-486
6. H. J. Snaith and M. Grätzel, *Appl. Phys. Lett.* 89, 262114, 2006.
7. D. Poplavskyy and J. Nelson, *J. Appl. Phys.* 93, 341 (2003).
8. N. D. Treat, N. Yaacobi-Gross, H. Faber, A.K. Perumal, D. D. C. Bradley, N. Stingelin, and T. D. Anthopoulos, *Appl. Phys. Lett.* 107, 013301 (2015).

Table S4 Literature survey of highly-efficient PSCs based on different HTM and ETLs

Perovskite absorber	ETL	HTL	PCE (%)	Stability (Hours)	Remark	Reference
$\text{CsI}_{0.05}(\text{FAPbI}_3)_{0.85}(\text{MAPbBr}_3)_{0.15}$	mp-TiO ₂	CuSCN (no additives)	20.4	1000 @ 85 °C >95% retention	Spin coated CuSCN with rGO interfacial layer	Science 358, 768–771 (2017)
$(\text{FAPbI}_3)_{0.85}(\text{MAPbBr}_3)_{0.15}$	PCBM/ZnO	np-NiOx	19.10	N/A	PCBM/ZnO window complicated and short deposition window	Materials Today 2018, 21, 483-500
$\text{Cs}_{0.05}\text{MA}_{0.95}\text{PbI}_3$	PCBM/BCP/AZO	NiOx	18.45	500 @ 85 °C	86.7 % retention and ALD process is expensive	Adv. Mater. 2018, 30, 1801010
$(\text{FAPbI}_3)_{0.95}(\text{MAPbBr}_3)_{0.05}$	mp-TiO ₂	DM (additives doping needed)	23.2	120 @ 85 °C 500 @ 60 °C	Newly designed HTM from complicated process and containing additives doping	Nature Energy (2018) https://doi.org/10.1038/s41560-018-0200-6
$(\text{PEA})_2(\text{MA})_2\text{Pb}_3\text{I}_{10}$	mp-TiO ₂	PTAA (additives doping needed)	20.1	760 @ 85 °C	OA and PEA modified perovskite with PTAA additives doped HTM	Energy Environ. Sci., 2018, 11, 2188
$\text{Rb}_5\text{Cs}_{10}\text{FAPbI}_3$	mp-TiO ₂	Spiro-MeOTAD (additives doping needed)	20.35	18.16 after 1000 hours at 85 °C	MA-free perovskite with additives doped HTM	Science 10.1126/science.aat3583 (2018).

$\text{CsI}_{0.05}(\text{FAPbI}_3)_{0.85}(\text{MAPbBr}_3)_{0.15}$	mp-TiO ₂	CuSCN (no additives)	18.78	>2000 hours at 85 °C	Developed air- processed smart bottle method for CuSCN HTM deposition	Present work